Evidence of refractive index variation with roughness in CLOUDSAT W-band radar and different applications of lidar/radar ocean surface echo

D. Josset[1], J.Pelon[2], Y. Hu[3], S. Tanelli[4], C.Trepte[3], P.Zhai[5]

1 NASA Postdoctoral Program, 2 IPSL/LATMOS, 3 NASA LaRC Climate branch, 4 NASA JPL, 5 SSAI

1. INTRODUCTION

Lidar and radar observations from CALIPSO and CloudSat missions have allowed the development of methods to determine atmospheric parameters [1, 2]. Total aerosol optical depth (AOD) and cloud liquid water path have thus been derived at the scale of the lidar or radar footprint using AMSR-E wind speed information [3, 4], or the combination of lidar and radar observations using ocean surface echo[5]. We present here the relationship between the wind speed retrieved by AMSR-E radiometer and the normalized scattering cross section of the radar (CPR) in cloud free regions [6]. We also discuss the potential improvement for lidar and radar calibration and the value of collocated lidar/radar ocean surface observations to study the different way to correct CLOUDSAT from water vapor attenuation.

2. RADAR OCEAN SURFACE ECHO

The attenuated normalized radar surface scattering cross section $\sigma_{SR,att}$ over the ocean for a nadir pointing can be written as [5]

$$\sigma_{SR,att} = C_R \frac{\rho_{0R}}{< S^2 >_R} T_{AR}^2 = \sigma_{SR} T_{AR}^2 \qquad (1)$$

where the subscript S denotes the surface; R stands for radar measurements; att means attenuated. $<S^2>_R$ is the variance of the slope distribution of the ocean surface waves induced by wind. ρ_{0R} is the Fresnel reflectance coefficient assuming a 35‰ ocean salinity and T^2_{AR} (subscript A for atmosphere) is the two-way atmospheric transmission at radar wavelength. C_R and $<S^2>_R$ take into account the diffraction induced by the size of the scattering elements of the surface waves relative to the measurement wavelength, and more generally, the spectral cut induced by the observed variance of waves and refraction coefficient [7, 12, 14].

3. RADAR MEAN SQUARE SLOPE ANALYSIS

The ocean surface model we have used [12, 21] allows to model both radar and lidar as a function of wind speed, which can be applied to collocated CLOUDSAT and AMSR-E observations. We present here the results for 1

month of observations of the ocean surface over the globe using CLOUDSAT Level 1 R04 data. Radar operational normalized scattering cross section has been linearized. When scaling the radar surface signal at global scale, ocean temperature dependence of the refractive index needs to be taken into account [7]. ρ_{0R} variations with sea surface temperature have been taken into account using [8] and AMSR-E measurement. Liebe's model [9] is used for water vapor attenuation correction. Attenuation at 94 GHz in clear air is due to oxygen and water vapor absorptions [9, 10]. The attenuation due to water vapor weakly depends on the shape of water vapor profile, and can be determined by the integrated water vapor path to the first order [5, 11]. In order to reduce the error sources and dispersion of the analysis, we forced the Global Modeling and Assimilation Office (GMAO) humidity profiles used in CALIPSO data analysis to be adjusted to the integrated water vapor path (IWVP) from AMSR-E with a multiplicative constant. This water vapor correction is expected to be precise to within 5% because it gives very similar retrievals to the method in [26] but we will discuss in part 4. how to improve it. For radar observations, the effective refractive coefficient will in fact depend on wind speed [14, 23, 24]. In this case, the expression of C_R is given by [25]:

$$C_R = \left|1 - F(\lambda, \varepsilon, D)\right|^2 \tag{6}$$

where F is a complex function of the sensor wavelength λ, the dielectric constant of the ocean ε, and the spectral energy density D of surface roughness. This function represents the amount of energy loss due to diffraction by surface roughness [25]. It is equal to 1 at low wind speed for a perfectly smooth surface [7, 23]. We reported on Fig. 1 the apparent C_R determined by the ratio of the modelled mean square slope with AMSR-E wind speed measurements [12] and the best fit (centroid) of the radar collocated observations. Separating radar data between 1-15 and 15-31 August periods (E02 and E03) corresponding to off-nadir angle of 0° and 0.16° shows differences below 3 m/s. This is coming from the higher $\sigma_{SR,att}$ at true nadir observed by [26]. The change of slope as well as off nadir angle dependence is related to coherent scattering. Further data analysis is needed as well as new theoretical work addressing coherent scattering at 94GHz. One can see that the derived apparent C_R reported on Fig. 1 is increasing with decreasing wind speed, and becomes larger than 1.

As C_R coefficient should converge to 1 for a perfectly smooth surface at 0 wind speed, it can give us an estimation of the radar calibration bias. The exact value of calibration bias is dependent of Liu's model characteristics, especially the underlying wave spectrum. The exact shape of the F function will also change C_R accordingly. However as C_R is expected to decrease monotonically with wind speed, its value at 4 m/s can be used as a minimal estimation (0.53 ±0.5 dB). The calibration bias is within CLOUDSAT uncertainty, but a thorough data analysis using more measurements at lower wind speeds and theoretical studies has to be conducted to improve the estimate of the shape of F function, the effect of pointing change as well as the model accuracy. For the estimation of this study, we used the standard deviation of the CLOUDSAT data (Fig. 1) and retain an estimation of 1.43±1 dB.

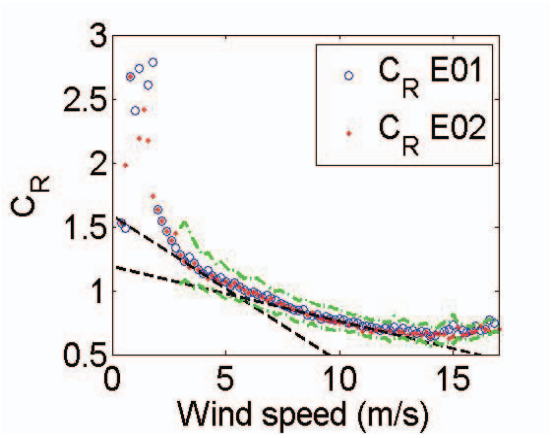

Fig. 1. : C_R coefficient as a function of wind speed that allows to take diffraction effect by capillary waves into account. Ratio of modelled $<S^2>_R$ with the distribution centroid of the expected $<S^2>_R$ (C_R=1) derived from the radar signal (corrected from attenuation) as a function of AMSR-E wind speed with different off-nadir angle (E01 and E02). Dashed lines correspond to curve gradients at 4 and 10 m/s and dash dotted shows the standard deviation of the data.

4. IMPROVEMENT OF WATER VAPOR CORRECTION

As we can see on Fig. 2 there is a well defined relationship between the radar and lidar ocean surface echo, but more important than that, their relative variations and error sources are uncorrelated because the wavelenght are different and they are on different platforms. Thus, studying the dispersion of Fig. 2 allows to determine which method of CLOUDSAT water vapor correction present the lowest relative error. We will present the underlying assumption behind this methodology and our results.

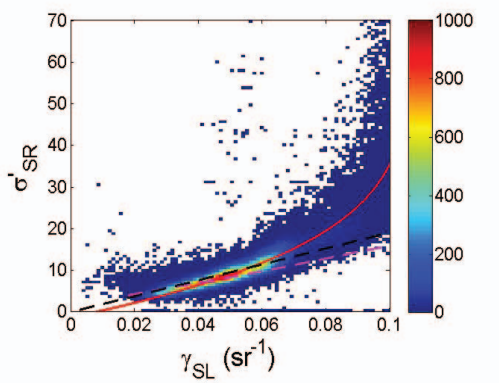

Fig. 2. Radar normalized cross section corrected from the refractive index temperature variations and water vapor as a function of lidar surface echo (corrected from molecular attenuation) for August 2006 nighttime in clear air. Color code represents the number of occurrences. The black dotted line corresponds to a linear adjustment as in [5]. The solid red line corresponds to the polynomial adjustment defined in [6]. $\sigma'_{SR} = 0.4\ \sigma_{SR}/\rho_{0R}$ (ρ_{0R} = 0.40 at the wavelengths of 3.1 mm and at 15°C).

5. CONCLUSION

We will present how we determined a possible bias on radar calibration but also the different applications concerning lidar calibration, improvement of CLOUDSAT water vapor correction and retrieval of geophysical properties like aerosol optical depth retrieval at lidar wavelength. We also propose to discuss the need for further work using the new observations at 94 GHZ and theoretical analysis that should be performed. This work has important applications for lidar and radar measurements from space platforms.

REFERENCES

[1] Winker, D. M., Pelon, J., and McCormick, M. P. (2003), The CALIPSO mission: Spaceborne lidar for observation of aerosols and clouds. *Proc. SPIE*, 4893, 1-11.

[2] Stephens G. L., D. G. Vane, S. Tanelli, E. Im, S. Durden, M. Rokey, D. Reinke, P. Partain, G. G. Mace, R. Austin, T. L'Ecuyer, J. Haynes, M. Lebsock, K. Suzuki, D. Waliser, D. Wu, J. Kay, A. Gettelman, Z. Wang, R. Marchand (2008), CloudSat mission: Performance and early science after the first year of operation, *J. Geophys. Res.*, doi:10.1029/2008JD009982.

[3] Hu, Y., Stamnes, K., Vaughan, M., Pelon, J., Weimer, C., Wu, D., Cisewski, M., Sun, W., Yang, P., Lin, B., Omar, A., Flittner, D., Hostetler, C., Trepte, C., Winker, D., Gibson, G., and Santa-Maria, M., Sea surface wind speed estimation from space-based lidar measurements, *Atmos. Chem. Phys. Discuss.*, 8, 2771-2793, 2008.

[4] L. D. H. Smith and A. J. Illingworth (2008), Global statistics of the liquid water path and drizzle occurrence in low level liquid water clouds derived from CloudSat using the attenuation of the ocean return. *15th international conference on clouds and precipitation (ICCP 2008)*, Cancun, Mexico, 7-11 July 2008

[5] Josset, D., J. Pelon, A. Protat, and C. Flamant, New approach to determine aerosol optical depth from combined CALIPSO and CloudSat ocean surface echoes, *Geophys. Res. Lett.*, 35, L10805, 2008. doi: 10.1029/2008GL033442

[6] Josset, D., J. Pelon, and Y. Hu, Multi-Instrument Calibration Method Based on a Multiwavelength Ocean Surface Model, IEEE GRSL, in press.

[7] Li, L., Heymsfield, G. M., Tian, L., and P. E. Racette (2005), Measurements of ocean surface backscattering using an airborne 94-GHz cloud radar – Implication for calibration of airborne and spaceborne W-Band Radars. *J. Atmos. Oceanic Technol.*, 22, 1033–1045.

[8] T. Meissner and F. J. Wentz (2004), The complex dielectric constant of pure and sea water from microwave satellite observations. *IEEE Trans. Geosc. Rem. Sens.,* 42 (9), 1836-1849

[9] Liebe, H. L. (1985), An updated model for millimetre wave propagation in moist air. *Rad. Sci.,* 20 (5), 1069-1089

[10] Lhermitte , R. (1987), A 94GHz Doppler Radar for cloud Observations. *J. Atmos. Oceanic Technol.*, 4, 36 – 48.

[11] Wentz, F. J., http://www.eorc.jaxa.jp/sharaku/AMSR/doc/alg/5_alg.pdf , AMSR ocean algorithm, AMSR ATBD

[12] Liu, Y., Su, M. Y., Yan, X. H. and W. T. Liu (2000), The mean-square slope of ocean surface waves and its effect on radar backscatter. *J. Atmos. Oceanic Technol.*, 22, 1033–1045

[13] Cox, C., and W. Munk (1954), Measurement of the Roughness of the sea surface from photographs of the sun's glitter. *J. Opt. Soc. Am.*, 44 (11), 838–850.

[14] Valenzuela R. G. (1978), Theories for the interaction of electromagnetic and oceanic waves – a review. *Boundary Layer Meteorology,* (13), 61-85

[15] Koepke, P. (1984), Effective reflectance of oceanic whitecaps, *Appl. Opt.*, 23, 1816 – 1824.

[16] Flamant, C., Pelon, J., Hauser, D., Quentin, C., Drennan, W. M., Gohin, F., Chapron B., and J. Gourrion (2003), Analysis of surface wind speed and roughness length evolution with fetch using a combination of airborne lidar and radar measurements. *J. Geophys. Res.*, 108 (C3), 8058.

[17] Shaw, J. A. and J. H. Churnside (1997), Scanning-laser glint measurements of sea-surface slope statistics, *Appl. Opt.*, 36, 4202 – 4213.

[18] Phillips, O. M. (1977), The dynamic of the upper ocean, 2nd ed. Cambridge University Press

[19] Bufton, J. L., Hoge, F. E. and R. N. Swift (1983), Airborne measurements of laser backscatter from the ocean surface, *Appl. Opt.*, 22 (17), 2603–2618.

[20] Apel, J. R. (1994), An improved model of the ocean surface wave vector and its effect on radar backscatter. *J. Geophys. Res.,* 99, 16,269–16,291

[21] Liu, Y., Yan, X. H., Liu, W. T. and P. A. Hwang (1997), The probability density function of ocean surface slopes and its effect on radar backscatter. *J. Phys. Ocean.*, 22, 1033–1045

[22] Kaufman Y. J., A. Smirnov, B. N. Holben and O. Dubovik (2001), Baseline maritime aerosol: methodology to derive the optical thickness and scattering properties. *Geophys. Res. Lett.*, 28, 3251-3254.

[23] Jackson, F. C., Walton, W. T., Hines, D. E., Walter, B. A. and C. Y. Peng (1992), Sea surface mean square slope from Ku-Band backscatter data. *J. Geophys. Res.*, 97 (C7), 11411–11427.

[24] Freilich, M. H. and B. A. Vanhoff (2003), The relationship between winds, surface roughness, and radar backscatter at low incidence angles from TRMM precipitation radar measurements. J. Atm. Ocean. Tech.

[25] Valenzuela, G. R. (1970), The Effective Reflection Coefficients in Forward Scattering from a Dielectric Slightly Rough Surface, *IEEE Proc.*, 58, 1279.

[26] S. Tanelli, S. L. Durden, E. Im, K. S. Pak, D. G. Reinke, P. Partain, J. M. Haynes and R. T. Marchand (2008), Cloudsat's Cloud Profiling Radar after two years in Orbit: Performance, Calibration and Processing, *IEEE Trans. Geosc. Rem. Sens.,* 46 (11), 3560-3573